— Supporting information —

Fluorescent secreted bacterial effectors reveal active intravacuolar proliferation of *Listeria monocytogenes* in epithelial cells

Caroline Peron-Cane[1,2], José-Carlos Fernandez[2], Julien Leblanc[2], Laure Wingertsmann[2], Arnaud Gautier[3,4], Nicolas Desprat[1,2,5,*] and Alice Lebreton[2,6,*]

[1] Laboratoire de Physique de l'École normale supérieure, ENS, Université PSL, CNRS, Sorbonne Université, Université de Paris, 75005 Paris, France.

[2] Institut de biologie de l'ENS (IBENS), École normale supérieure, CNRS, INSERM, Université PSL, 75005 Paris, France.

[3] Sorbonne Université, École normale supérieure, Université PSL, CNRS, Laboratoire des Biomolécules, LBM, 75005 Paris, France.

[4] Institut Universitaire de France.

[5] UFR de Physique, Université Paris-Diderot, Université de Paris, 75005 Paris, France.

[6] INRAE, IBENS, 75005 Paris, France.

[*] For correspondence: alice.lebreton@ens.psl.eu; nicolas.desprat@ens.psl.eu

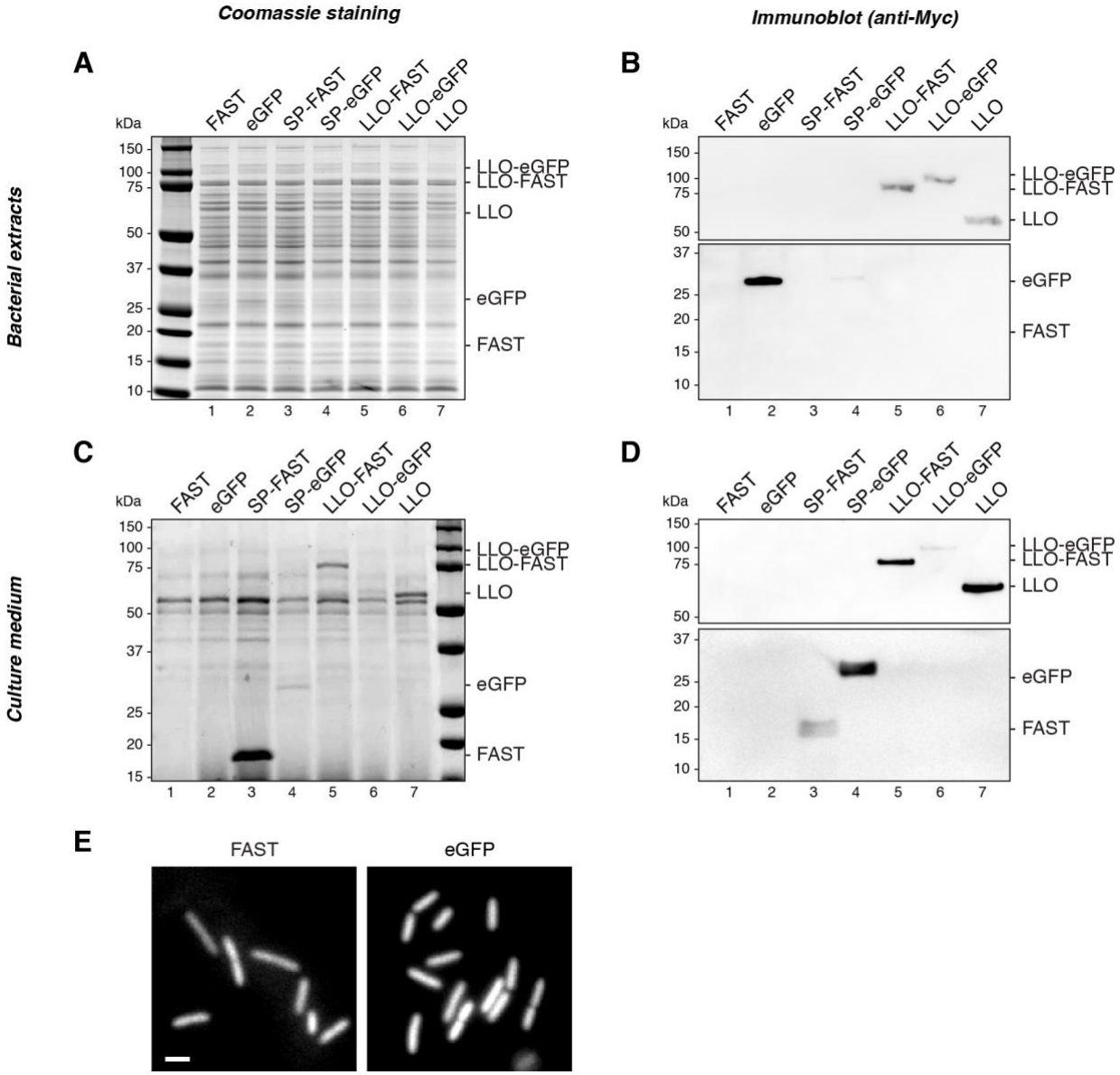

S1 Fig. Production and secretion of the Myc-tagged fusion proteins by *Listeria monocytogenes* LL195.

Protein production and secretion of Myc-tagged fusion proteins for each one of the constructs described in Fig 1A (constitutive expression from an integrated pAD vector) was assessed by colloidal Coomassie staining (**A, C**) and immunoblotting with anti-Myc antibodies (**B, D**) of bacterial total extracts (**A, B**) and culture supernatant fractions (**C, D**) from 16-h cultures in BHI, separated by SDS-PAGE.

(**E**) Epifluorescence microscopy observation of strains producing non-secreted FAST or eGFP. Scale bar, 2 μm.

Most Myc-tagged protein constructs were detected by immunoblotting in the corresponding bacterial pellet fraction, indicating that transgenes were expressed, even though in varying amounts (**B**, lanes 2, 4-7). Constructs harbouring the LLO SP or full-length LLO were recovered in bacterial supernatants (**C, D**, lanes 3-7), suggesting that the SP of LLO promoted Sec-dependent export of not only of FAST or FAST-tagged proteins, but also of eGFP-fusion proteins. The secretion of eGFP-tagged proteins seemed less efficient than that of FAST-tagged protein (**C**, compare lane 3 with 4; **D**, compare lane 5 with 6), consistent with previous reports that eGFP is a poor substrate for Sec-dependent secretion[18]. Constructs devoid of signal peptides were not detected in supernatant fractions (**C, D**, lanes 1-2), arguing against the release of proteins into the culture medium due to bacterial lysis.

For technical reasons likely due to the small size of FAST-Myc (15 kDa), it was not or barely detected by immunoblotting (**B, D**, lanes 1, 3); nevertheless, a strong signal corresponding to this polypeptide was visible on Coomassie-stained gels of the supernatant fractions, attesting of its secretion (**C**, lane 3). For bacterial pellet fractions (**A**, lanes 1, 3), signal from other proteins masked possible bands from that polypeptide; however, observation in microscopy (**E**) confirmed the non-secreted form of FAST was also produced.

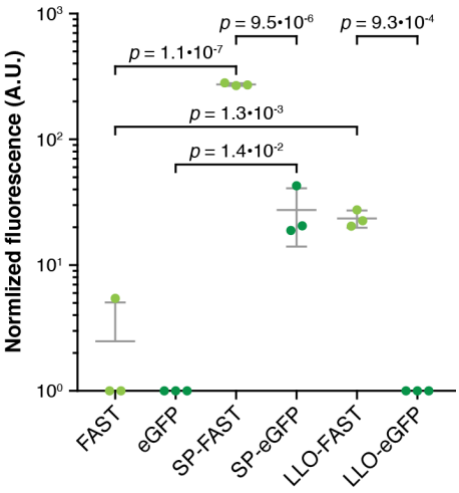

S2 Fig. Fluorescent measurements of FAST- or eGFP-tagged proteins released in bacterial culture supernatants.

Six *Lm* strains expressing FAST- or eGFP-tagged proteins were cultured in LSM, then fluorescence intensities were measured on the filtered supernatants of each culture in presence of 5 µM HBR-3,5DM. For normalisation between FAST and eGFP signals, intensities were expressed in arbitrary units where 100 A.U. corresponds, for each reporter, to the intrabacterial fluorescence emitted by a suspension of equal volume of *Lm* (OD_{600nm} = 1) that expresses constitutively either non-secreted FAST or eGFP under the P_{HYPER} promoter. Residual fluorescence measured in the culture medium of strains producing non-secreted FAST or eGFP represents bacterial lysis. All values below 1 were considered below the detection limit for this experiment, and plotted as 1 (*i.e.* 10^0). Normalized values, means and standard deviations from three independent experiments were plotted. *p*-values represent the results of two-tailed Student's *t*-tests with equal variance assumption.

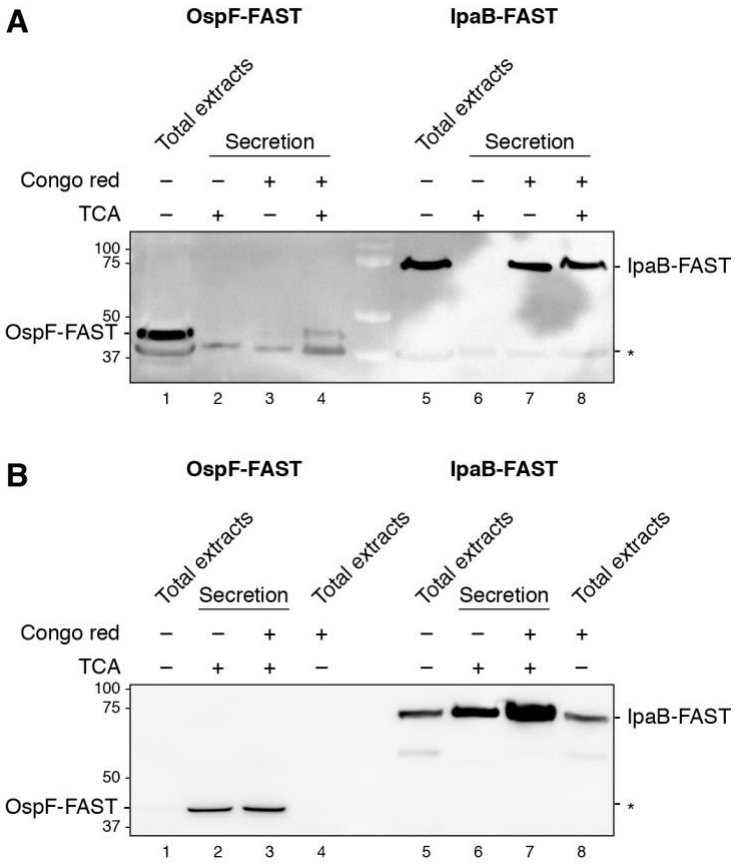

S3 Fig. Production and secretion of the Myc-tagged fusion proteins by *Shigella flexneri* M90T.

Protein production and secretion of Myc-tagged fusion proteins for each one of the constructs described in Fig 1C (constitutive expression from a pSU2.1rp vector) was assessed by immunoblotting with anti-Myc antibodies of bacterial total extracts culture supernatant fractions, with or without induction of secretion by the T3SS using Congo red, and with or without TCA precipitation in order to concentrate samples.

(**A**) Samples from wild type M90T *Sf*.

(**B**) Samples from M90T Δ*ipaD*, in which T3SS secretion is constitutive. *, non-specific band.

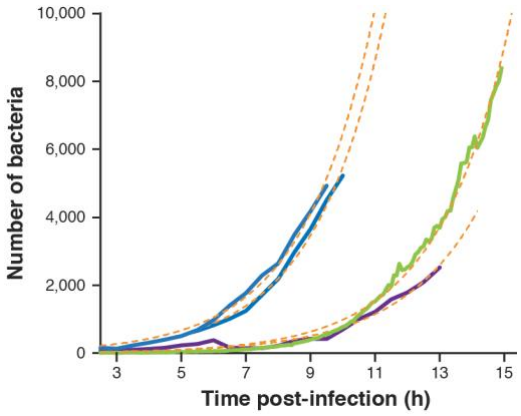

S4 Fig. Exponential growth of mCherry-labelled bacteria in infected LoVo cells.

Dynamics of the total intracellular bacterial population were measured by segmentation of mCherry-labelled bacteria, in control wells recorded in parallel to the accumulation of SP-FAST in the cytoplasm (Fig 2). To get an estimate of the number of bacteria in each field, the total volume occupied by bacteria (the number of voxels that were labelled with mCherry) was divided by the average size of bacteria (32 voxels). Each colour represents an independent biological replicate (in blue, two wells were recorded in the same experiment). The exponential fit associated to each growth curve is displayed as orange dashed lines.

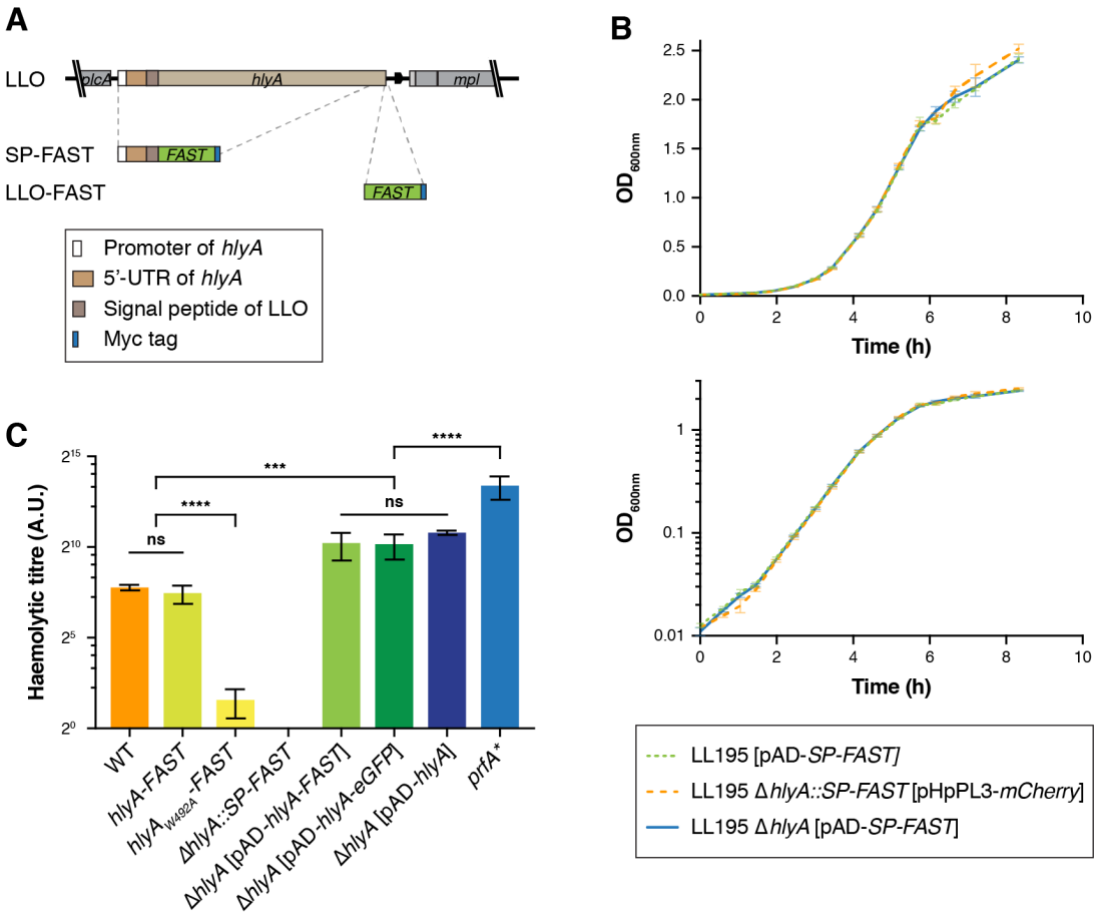

S5 Fig. Construction, growth and haemolytic properties of the main *Lm* strains used in this study.

(**A**) Diagram of allelic replacement of *hlyA* (encoding LLO) at its chromosomal locus by a cassette expressing *SP-FAST* under the endogenous *hlyA* promoter (Δ*hlyA::SP-FAST*), and of in-frame C-terminal tagging of LLO with FAST (*hlyA-FAST*).

(**B**) Growth curves of three *Lm* LL195 strains harbouring pPL2-derived vectors, at 37°C in BHI. No differences in growth rates were detected, regardless of the pPL2-derived plasmid that was integrated at the $tRNA^{Arg}$ locus (pAD-*SP-FAST* or pHpPL3-*mCherry*) and of the genetic modification carried out at the *hlyA* locus (Δ*hlyA* or Δ*hlyA::SP-FAST*). Curves represent the average and standard deviation of technical triplicates, displayed in linear scale (top) or in semi-log scale (bottom).

(**C**) Haemolytic properties of the *Lm* strains producing FAST– or eGFP–tagged LLO fusions used in this study. The haemolytic titre measured for the strain where LLO was C-terminally tagged with FAST-Myc at the *hlyA* locus (*hlyA-FAST*) did not differ from that of the WT *Lm* strain. The haemolytic titre of all Δ*hlyA* strains was null (here, only Δ*hlyA::SP-FAST* was plotted). Haemolytic titres were enhanced for Δ*hlyA* deletion strains that had been complemented by integrative pAD plasmids harbouring *hlyA* fusion genes under control of the constitutive P_{HYPER} promoter. Fusion with FAST-Myc or eGFP-Myc (pAD-*hlyA-FAST* or *-eGFP*) did not affect haemolytic properties, compared to a simple fusion with Myc (pAD-*hlyA*). None of these strains reached the intense haemolytic properties of the *prfA** strain (48.9-fold above the WT strain), for which the expression of *Lm* virulence genes (including *hlyA*) is deregulated, due to the constitutive activity of the transcriptional activator PrfA [22]. The average haemolytic titres and standard deviations from three independent experiments were plotted. Two-way ANOVA on $\log_2$-transformed haemolytic titres followed by post-hoc Tukey's test was used for statistical testing between conditions. ns, non-significant; ***, $p < 10^{-3}$, ****, $p < 10^{-4}$.

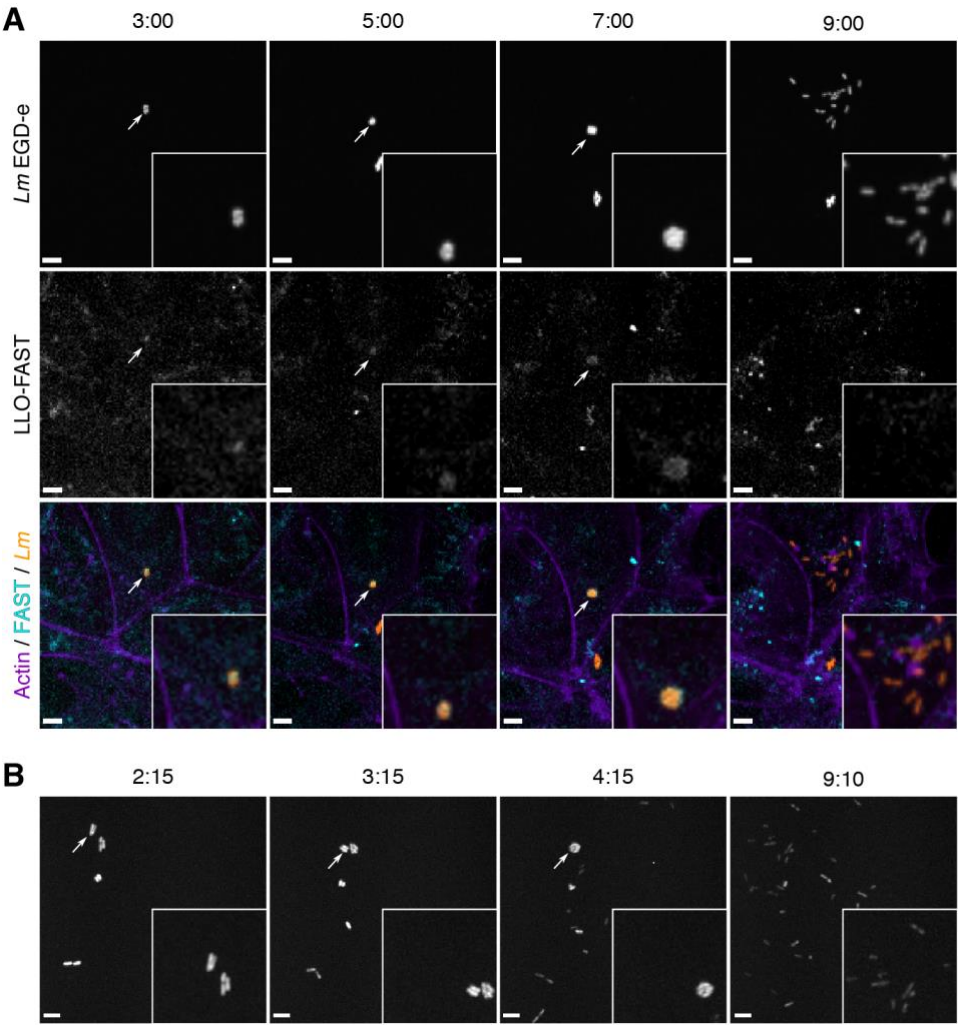

S6 Fig. Proliferation of *Lm* inside vacuoles when using the EGD-e strain in LoVo cells, or the LL195 strain in Caco-2 cells.

(**A**) LoVo cells infected with *Lm* EGD-e expressing both mCherry and LLO-FAST were observed between 2 and 8 h post-infection by spinning disk confocal microscopy. On the merged image, LLO-FAST is in cyan, mCherry is in orange, and SiR-actin is in purple.

(**B**) Time-course of replication of mCherry-expressing *Lm* LL195 inside a vacuole, observed in the Caco-2 cell line.

(**A, B**) Scale bars, 5 μm; timescale, h:min.

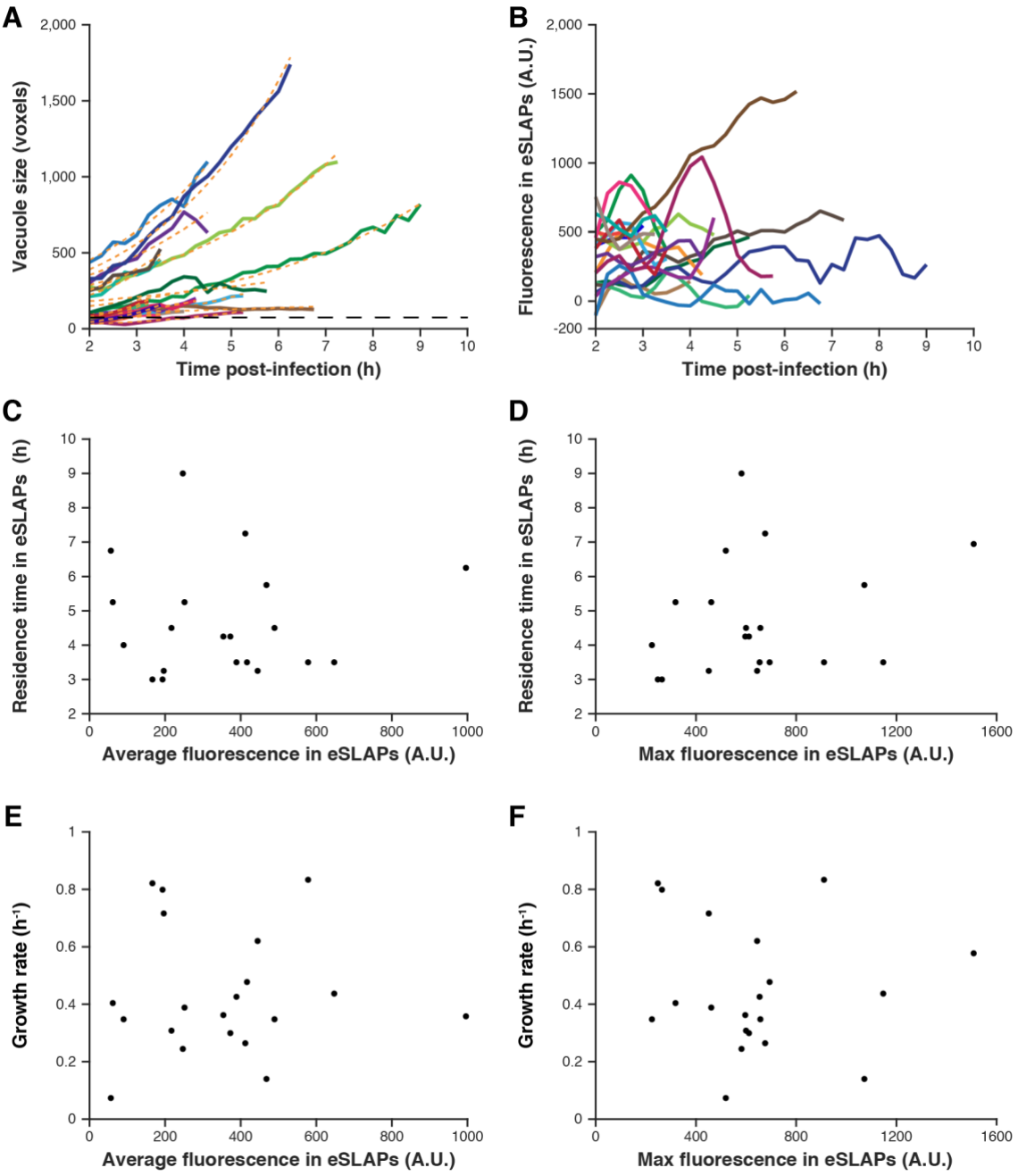

S7 Fig. Quantitative and correlative analysis of the growth of bacteria and the secretion of LLO-FAST in eSLAPs over time.

LoVo cells were infected with *Lm* carrying an integrated pHpPL3-*mCherry* plasmid and secreting FAST-LLO due to an in-frame C-terminal fusion with FAST at the *hlyA* locus.

(**A**) Number of bacteria inside eSLAPs over time. mCherry signals allowed the segmentation of bacteria and their counting. The exponential fit associated to each growth curve is displayed as orange dashed lines. The black horizontal dashed line represents the volume of one average doubling event since the first frame.

(**B**) Quantification of the fluorescence over time in the FAST channel, which reports for the concentration of LLO-FAST in eSLAPs.

(**C-F**) Correlation between the fluorescence generated by LLO-FAST in eSLAPs and either the time residence time or the growth rate in these compartments. The average intensity of fluorescence generated by the secretion of LLO-FAST (**C, E**) and the maximum intensity of LLO-FAST fluorescence (**D, F**) were extracted for each eSLAP (n = 21) and correlated with the duration of this compartment since the beginning

of acquisition (**C, D**) or with the growth rate of bacteria in this compartment, defined by the rate of increase of the size of the mCherry-labelled volume occupied by intravacuolar bacteria (**E, F**).

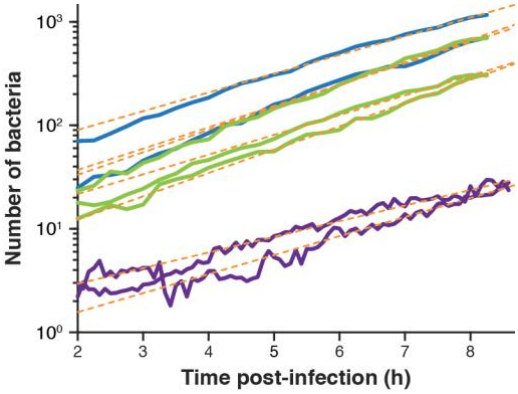

S8 Fig. Growth of *Lm hlyA-FAST* [pHpPL3-*mCherry*] in infected LoVo cells.

The number of mCherry-labelled bacteria was determined by segmenting the volume they occupied, as in S4 Fig. Each colour represents an independent biological replicate. Curves of the same colour represent technical replicates. The exponential fit (linear fit in semi-log scale) associated to each growth curve is displayed as orange dashed lines.

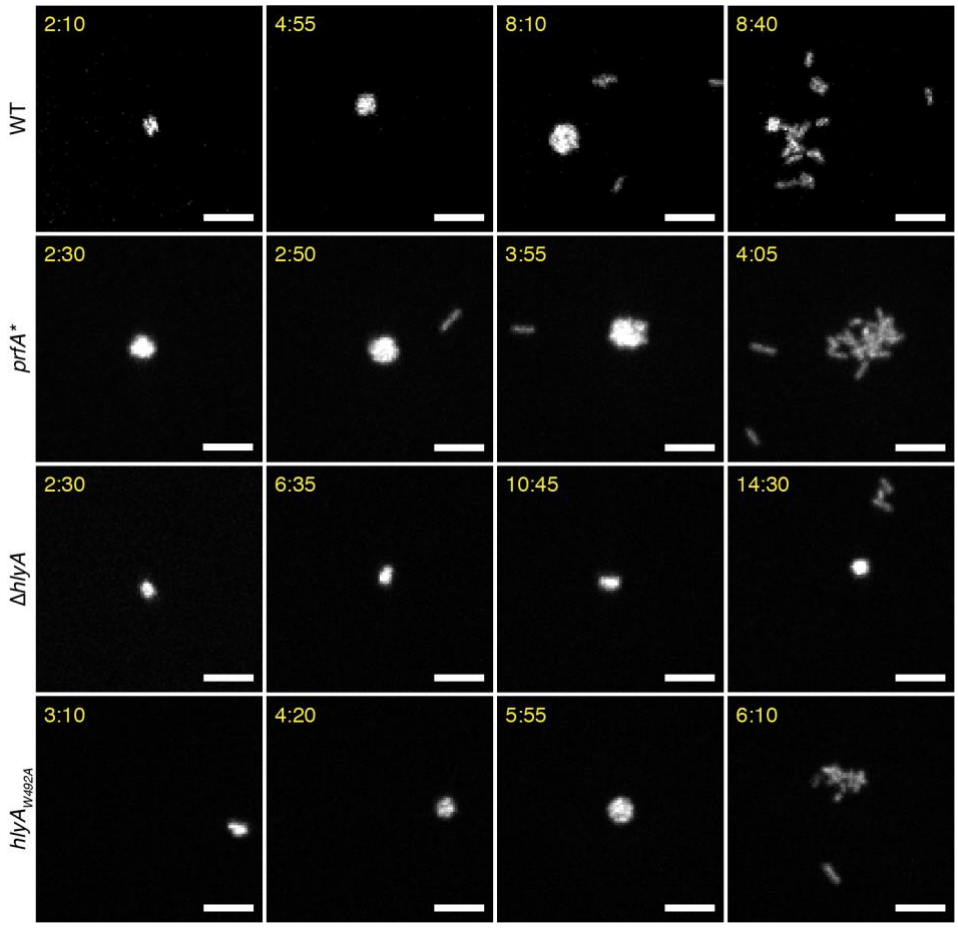

S9 Fig. Time-course of replication of mCherry-expressing *Lm* inside eSLAPs for WT, *prfA Δ*hlyA* and *hlyA*$_{W492A}$ *Lm* during the infection of LoVo cells.**

The fluorescent signal of mCherry expressed constitutively was used to locate bacteria. Bacteria that were confined in eSLAPs were packed in a spherical configuration and observed as large spots on fluorescence images. When the vacuole ruptured, membrane tension was released and bacteria dispersed into the cytoplasm. Scale bars, 5 μm; timescale, h:min.

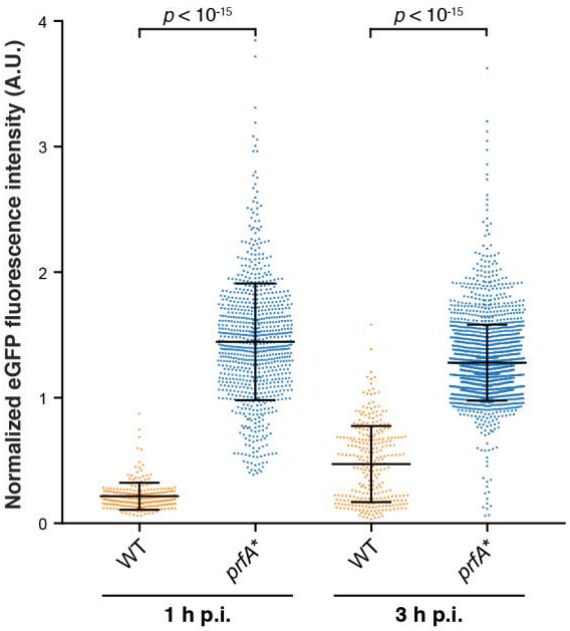

S10 Fig. Expression of eGFP driven by the P_{hlyA} promoter in intracellular WT or *prfA bacteria.**

LoVo cells infected with either WT or *prfA** EGD-e *Lm* strains, where eGFP was in transcriptional fusion with the promoter of *hlyA* by chromosomal allelic replacement (Δ*hlyA::eGFP*), and co-expressing mCherry. Data represent the ratio of eGFP to mCherry signals for each segmented bacterium. The number of analysed bacteria per condition was n = 234 for WT and n = 846 for *prfA** bacteria at 1 h p.i.; n = 289 for WT and n = 2,124 for *prfA** bacteria at 3 h p.i. Means and standard deviations are represented in black solid lines. Note that the distribution of intensities was bimodal for the WT strain at 3 h p.i., likely reflecting the induction of P_{hlyA} in some, but not all of the bacteria at this stage. *p*-values indicate the results of Kruskal-Wallis non-parametric test followed by Dunn's correction for multiple testing.

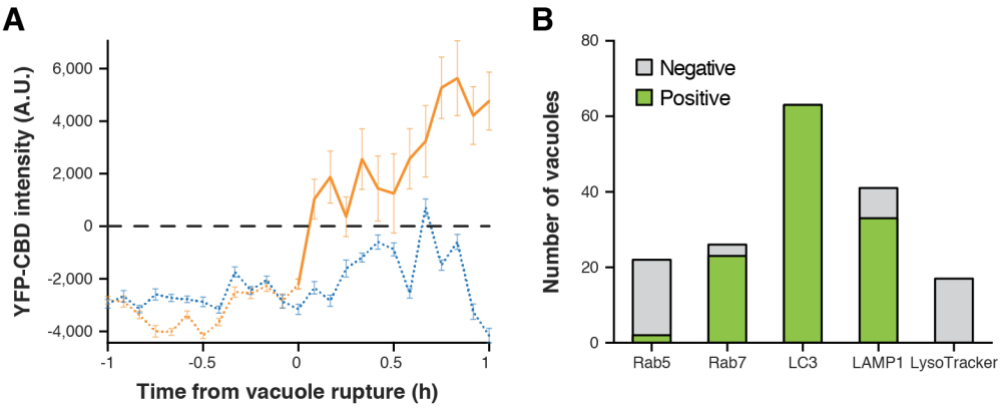

S11 Fig. Quantification of the co-localisation of eSLAPs with YFP-CBD and with markers of endosome maturation.

(**A**) YFP fluorescence intensity (reporting for the exposure of *Lm* to the host cytoplasm) was measured in bacteria before (dotted lines) or after (solid line) their release from eSLAPs, in the cell shown in Fig 5A and Movie S5. The average background signal from the cytosol was subtracted and is represented as a black dashed line at 0 A.U. The orange trace displays the fate of a vacuole (dotted line) that ruptured at time 0 and released 11 bacteria (solid line) into the host cytosol. The blue trace represents a control vacuole in the same cell that did not rupture over the same time-course. Negative values correspond to signals below cytosolic levels, indicating that YFP-CBD was excluded from eSLAPs when they formed. In contrast, when bacteria were exposed to the host cytosol, they became positively stained. Error bars indicate the standard error of the mean.

(**B**) The co-localisation of Rab5, Rab7, LC3 and LAMP1 with eSLAPs containing mCherry-labelled bacteria (immunofluorescence), or of LysoTracker Deep-red with GFP-labelled bacteria (live imaging), was assessed on infected LoVo cells at 3 h p.i. The occurrence of co-localisation events was 9% for Rab5 (2/22), 88,5% for Rab7 (23/26), 100% for LC3 (63/63), 80,5% for LAMP1 (33/41) and null for LysoTracker (0/17).

A *EagI*-5'-UTR$_{hlyA}$-SP$_{hlyA}$-FAST$_{Lm}$-Myc-STOP-*SalI*

tgtgt***CGGCCG***ataaagcaagcatataatattgcgtttcatctttagaag
cgaatttcgccaatattataattatcaaaagagaggggtggcaaacggta
tttggcattattaggttaaaaaatgtagaaggagagtgaaacccATGAAA
AAAATAATGCTAGTTTTTATTACACTTATATTAGTTAGTCTACCAATTGC
GCAACAAACTGAAGCAAAGGATGAACATGTTGCTTTCGGTTCTGAAGATA
TCGAAAATACACTTGCAAAAATGGATGATGGTCAACTTGATGGCCTAGCA
TTCGGTGCTATTCAACTTGACGGCGACGGCAACATTCTTCAATACAACGC
GGCAGAAGGAGATATTACTGGTCGTGATCCAAAACAAGTAATTGGAAAAA
ACTTTTTCAAAGACGTTGCTCCAGGGACCGATAGCCCTGAATTCTATGGA
AAATTTAAAGAAGGTGTAGCTTCTGGCAATCTAAACACTATGTTCGAATG
GATGATCCCAACATCACGTGGACCAACAAAAGTTAAAGTTCATATGAAAA
AAGCACTAAGCGGAGATTCATATTGGGTTTTTGTTAAACGTGTAgaacaa
aaacttatcagcgaagaagatttaTAA***GTCGAC***ctcgaggggggcccgg
taccagctt

B *BamHI*-FAST$_{Sf}$-Myc-STOP-*XbaI*

ATG***ggatcc***GAACATGTTGCGTTCGGCAGCGAAGATATTGAGAACACCTT
AGCTAAAATGGACGATGGTCAGTTAGACGGCCTGGCTTTTGGTGCGATCC
AGCTGGACGGCGACGGCAACATCCTGCAGTACAACGCGGCTGAAGGTGAT
ATCACCGGTCGCGATCCGAAACAGGTGATCGGCAAAAACTTCTTCAAAGA
CGTTGCGCCGGGTACTGACTCTCCGGAATTCTACGGTAAATTTAAAGAGG
GTGTCGCGTCCGGTAACCTGAACACCATGTTCGAATGGATGATCCCAACC
TCCCGCGGCCCAACCAAAGTTAAAGTCCACATGAAAAAAGCACTGAGCGG
CGATTCTTATTGGGTGTTCGTTAAACGTGTTgaacagaaactgatctctg
aggaagatctgTAA***tctaga***gtcg

S12 Fig. Synthetic gene fragments with codon-optimized sequences for expression of FAST fusions in (A) *Listeria monocytogenes* (*Lm*) or (B) *Shigella flexneri* (*Sf*).

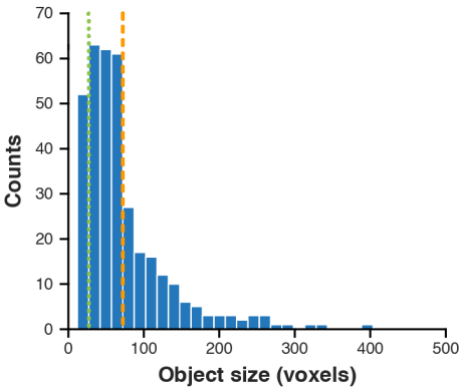

S13 Fig. Distribution of object sizes on the first frames of time-lapses during the infection of LoVo cells by mCherry-labelled bacteria.

The first bin of the distribution (left of the green dotted line) corresponds to objects smaller than the size of bacteria that were discarded when counting the number of entry events. The bins between the green dotted and orange dashed lines correspond to single bacteria, the size of which was in the range of 32 to 64 voxels. The orange dashed line marks the limit between objects that correspond to individual bacteria (left) and clusters of bacteria (right). The mean of the distribution (n = 354 objects from 15 pooled experiments) was equal to 75 voxels.

S1 Movie. Accumulation of secreted FAST in the cytoplasm of infected cells.

LoVo cells infected with *Lm* expressing SP-FAST were observed between 2 and 14 h post-infection by spinning-disk microscopy. Scale bar, 10 µm.

S2 Movie. Observation of secreted FAST signals in *Listeria* entry vacuoles.

LoVo cells infected with *Lm* expressing mCherry (A) or mCherry and SP-FAST (B) were observed between 0 and 3.25 h post-infection by spinning-disk microscopy. Green, FAST channel (non-specific signals in A; secreted FAST in B); red, mCherry channel; blue, SiR-actin channel. Tracks for individual internalisation vacuoles containing mCherry-bacteria and SP-FAST are displayed in yellow. Scale bar, 10 µm.

S3 Movie. Observation of the decoration of vacuoles by LLO-FAST in *Listeria* cells infected by *Lm* LL195.

LoVo cells infected with *Lm* LL195 expressing both mCherry and LLO-FAST were observed between 2 and 8 h post-infection by spinning disk microscopy. Orange, FAST channel; cyan, mCherry channel; purple, SiR-actin channel. Scale bar, 5 µm.

S4 Movie. Observation of the decoration of vacuoles by LLO-FAST in *Listeria* cells infected by *Lm* EGD-e.

LoVo cells infected with *Lm* EGD-e expressing both mCherry and LLO-FAST were observed between 2 and 9 h post-infection by spinning disk microscopy. Orange, FAST channel; cyan, mCherry channel; purple, SiR-actin channel. Scale bar, 5 µm.

S5 Movie. Imaging of the differential labelling by CBD-YFP of the cytosolic *versus* intravacuolar populations of intracellular bacteria.

LoVo cells were transfected with pEYFP-CBD 24 h being infected with *Lm* expressing mCherry, then imaged by spinning disk microscopy from 2 to 8 h p.i. Cyan, CBD-YFP channel; Orange, mCherry channel. The cell outline is shown with a purple dashed line. Scale bar, 5 µm.

S1 Table. Bacterial strains.

Strain	Description	Reference
LL195	*L. monocytogenes* LL195	[39]
BUG1600	*L. monocytogenes* EGD-e	[41]
BUG2479	*E. coli* DH5α *[pAD-cGFP]*	[44]
AG87	*E. coli* Rosetta(DE3)pLysS [pET28a-*FAST*]	[17]
FXCV1	*E. coli DH5α [pSU2.1rp-mCherry]*	[47]
JDS1	*E. coli* SM10 [pHpPL3-*mCherry*]	[45]
M90T	*S. flexneri* M90T	[40]
SF622	*S. flexneri* M90T Δ*ipaD*	[50]
BIRD8	*E. coli* NEB5α [pAD-*SP-FAST-Myc*][†]	This work
BIRD9	*E. coli* NEB5α [pAD-*hlyA-Myc*]	This work
BIRD13	*L. monocytogenes* LL195 [pAD-*SP-FAST-Myc*]	This work

[†] All pAD constructs contain the P_{HYPER} constitutive promoter, the 5'-UTR of the *hlyA* gene, and the desired fusion protein. To simplify reading, the C-terminal Myc tag of constructs is not included in the plasmid names in the main text.

Strain	Description	Reference
BIRD14	*L. monocytogenes* LL195 [pAD-*hlyA-Myc*]	This work
BIRD15	*E. coli* NEB5α [pAD-*FAST*]	This work
BIRD16	*L. monocytogenes* LL195 [pAD-*FAST-Myc*]	This work
BIRD17	*E. coli NEB5α [pAD-eGFP-Myc]*	This work
BIRD18	*L. monocytogenes* LL195 [pAD-*eGFP-Myc*]	This work
BIRD19	*E. coli NEB5α [pAD-SP-eGFP-Myc]*	This work
BIRD20	*L. monocytogenes* LL195 [pAD-*SP-eGFP-Myc*]	This work
BIRD32	*E. coli NEB5α [pAD-hlyA-FAST-Myc]*	This work
BIRD33	*E. coli NEB5α [pAD-hlyA-eGFP-Myc]*	This work
BIRD38	*L. monocytogenes* LL195 [pAD-*hlyA*-FAST-Myc]	This work
BIRD39	*L. monocytogenes* LL195 [pAD-*hlyA*-eGFP-Myc]	This work
BIRD62	*E. coli* NEB5α *[pSU2.1rp-ospF-FAST-Myc]*	This work
BIRD64	*E. coli* NEB5α *[pSU2.1rp-ipaB-FAST-Myc]*	This work
BIRD62	*E. coli* NEB5α *[pSU2.1rp-ospF-FAST-Myc]*	This work
BIRD64	*E. coli* NEB5α *[pSU2.1rp-ipaB-FAST-Myc]*	This work
BIRD66	*S. flexneri* M90T [pSU2.1rp-*ospF-FAST-Myc*]	This work
BIRD67	*S. flexneri* M90T [pSU2.1rp-*ipaB-FAST-Myc*]	This work
BIRD84	*S. flexneri* M90T Δ*ipaD* [pSU2.1rp-*ospF-FAST-Myc*]	This work
BIRD85	*S. flexneri M90T* Δ*ipaD* [pSU2.1rp-*ipaB-FAST-Myc*]	This work
BIRD127	*L. monocytogenes* LL195 Δ*hlyA*	This work
BIRD204	*E. coli* NEB5α *[pMAD-hlyA-FAST-Myc]*	This work
BIRD207	*L. monocytogenes* EGD-e *hlyA-FAST-Myc*	This work
BIRD213	*E. coli* NEB5α *[pMAD-*Δ*hlyA::SP-FAST-Myc]*	This work
BIRD214	*E. coli* NEB5α *[pMAD-*Δ*hlyA::eGFP-Myc]*	This work
BIRD217	*L. monocytogenes* LL195 [pHpPL3-*mCherry*]	This work
BIRD220	*L. monocytogenes* EGD-e *hlyA-FAST-Myc* [pHpPL3-*mCherry*]	This work
BIRD223	*L. monocytogenes* EGD-e Δ*hlyA::eGFP-Myc* [pHpPL3-*mCherry*]	This work
BIRD224	*L. monocytogenes* EGD-e *prfA** Δ*hlyA::eGFP-Myc* [pHpPL3-*mCherry*]	This work
BIRD234	*L. monocytogenes* LL195 *prfA**	This work
BIRD240	*L. monocytogenes* LL195 *hlyA-FAST-Myc*	This work
BIRD242	*L. monocytogenes* LL195 Δ*hlyA::SP-FAST-Myc*	This work
BIRD244	*L. monocytogenes* LL195 *hlyA-FAST-Myc* [pHpPL3-*mCherry*]	This work
BIRD250	*L. monocytogenes* LL195 Δ*hlyA* [pHpPL3-*mCherry*]	This work
BIRD251	*L. monocytogenes* LL195 *prfA** [pHpPL3-*mCherry*]	This work
BIRD252	*L. monocytogenes* LL195 Δ*hlyA::SP-FAST-Myc* [pHpPL3-*mCherry*]	This work
BIRD256	*L. monocytogenes* LL195 Δ*hlyA* [pAD-*FAST-Myc*]	This work
BIRD257	*L. monocytogenes* LL195 Δ*hlyA* [pAD-*SP-FAST-Myc*]	This work
BIRD258	*L. monocytogenes* LL195 Δ*hlyA* [pAD-*hlyA-FAST-Myc*]	This work
BIRD259	*L. monocytogenes* LL195 Δ*hlyA* [pAD-*eGFP-Myc*]	This work
BIRD260	*L. monocytogenes* LL195 Δ*hlyA* [pAD-*SP-eGFP-Myc*]	This work
BIRD261	*L. monocytogenes* LL195 Δ*hlyA* [pAD-*hlyA-eGFP-Myc*]	This work
BIRD262	*L. monocytogenes* LL195 Δ*hlyA* [pAD-*hlyA-Myc*]	This work
BIRD288	*E. coli* NEB5α *[pMAD-hlyA$_{W492A}$-FAST-Myc]*	This work
BIRD294	*L. monocytogenes* LL195 *hlyA$_{W492A}$-FAST-Myc* [pHpPL3-*mCherry*]	This work

S2 Table. Oligonucleotides.

Name	Description	Sequence	Reference
oAL543	*Eag*I-*UTR*$_{hlyA}$ fw	tgtgtCGGCCGataaagcaa	This work
oAL544	*Xho*I-*Sal*I-Myc rv	CCctcgagGTCGACTTAtaa	This work
oAL545	*FAST*-*UTR*$_{hlyA}$ rv‡	acatgttcCATGGGTTTCACTCTCCTTC	This work
oAL546	*UTR*$_{hlyA}$-*FAST* fw	tgaaacccATGGAACATGTTGCTTTCGG	This work
oAL547	Myc-*eGFP* rv	atttttgttcTTTGTATAGTTCATCCATGCC	This work
oAL548	*eGFP*-Myc fw	actatacaaaGAACAAAAATTAATCTCTGAA	This work
oAL549	*Eag*I-*UTR*$_{hlyA}$ fw	gtgtgtCGGCCGataaagcaagcatataatattgcg	This work
oAL550b	*Sal*I-Myc-*hlyA* rv	cgagGTCGACTTAtaaatcttcttcagagattaatt tttgTTCGATTGGATTATCTACTT	This work
oAL551b	*FAST*-*hlyA* rv	gcaacaTGTTCGATTGGATTATCTACTTTAT	This work
oAL552b	*hlyA*-*FAST* fw	ataatccaatcGAACATGTTGCTTTCGGTTC	This work
oAL553	*eGFP*-SP$_{hlyA}$ rv§	ctcctttactATCCTTTGCTTCAGTTTGTTG	This work
oAL554	*SP*$_{hlyA}$-*eGFP* fw	gcaaaggatAGTAAAGGAGAAGAACTTTTC	This work
oAL651	*hlyA*-*eGFP* rv	TCTCCTTTACTatgttcGATTGGATTATCTAC	This work
oAL652	*eGFP*-*hlyA* fw	CAATCgaacatAGTAAAGGAGAAGAACTTTTC	This work
oAL703	*Kpn*I-*ipaB* fw	ctcGGTACCaaggagtaattattATGCAT	This work
oAL704	*Bam*HI-*ipaB* rv	CATGTTCggatccAGCAGTAGTTTGTTGCAAAAT	This work
oAL705	*ospF*-*Bam*HI-*FAST* fw	GATAGAGggatccGAACATGTTGCGTTCGGCAG	This work
oAL706	*Xba*I-Myc rv	cgactctagaTTAcagatcttcctcagaga	This work
oAL707	*Kpn*I-*ospF* fw	ctcGGTACCagaggacgttttctATGCCC	This work
oAL708	*Bam*HI-*ospF* rv	TTCggatccCTCTATCATCAAACGATAAAAT	This work
oAL974	*Sal*I-*hlyA* fw	TCCATATGACgtcgacAGCATTTAAAGCTGTA	This work
oAL975	3' of *hlyA*-Myc rv	ttacttttacaaTTAtaaatcttcttcgctga	This work
oAL976	Myc-3' of *hlyA* fw	gaagatttaTAAttgtaaaagtaataaaaaattaag	This work
oAL977	*Bgl*II-*mpl* rv	TTAACTAGACagatctTTGTGGGTATCAGC	This work
oAL981	*Sal*I-*plcA* fw	TCCATATGACgtcgacACTCGGACCATTGTAG	This work
oAL984	*FAST*-*SP*$_{hly}$A rv	aaagcaacatgttcATCCTTTGCTTCAGTTTG	This work
oAL985	*SP*$_{hlyA}$-*FAST* fw	ggatGAACATGTTGCTTTCG	This work
oAL987	*eGFP* fw	gaaacccATGAGTAAAGGAG	This work
oAL1073	*hlyA*$_{W492A}$ fw	GGGAATGGgcGAGAACGGTAATTGATGACC	This work
oAL1074	*hlyA*$_{W492A}$ rv	taCCGTTCTCgcCCATTCCCAAGCTAAACC	This work

‡ *UTR*$_{hlyA}$ refers to the 5'-UTR of the *hlyA* gene, bringing a ribosome binding site (RBS) and used to enhance gene expression [51].

§ *SP*$_{hlyA}$ indicates to the sequence encoding the signal peptide from LLO (*hlyA* gene).

fw, forward strand; rv, reverse strand.